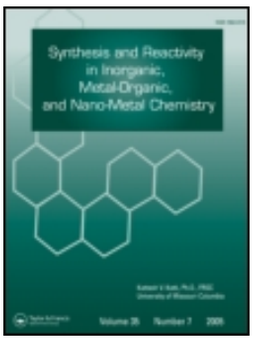

Synthesis and Reactivity in Inorganic, Metal-Organic, and Nano-Metal Chemistry

ISSN: 1553-3174 (Print) 1553-3182 (Online) Journal homepage: https://www.tandfonline.com/loi/lsrt20

3-Ethyl-4-amino-5-mercapto-1,2,4-triazole as a Corrosion Inhibitor for 6061/Al –15 vol% SiC_p Composite in a Sodium Hydroxide Solution

P. D. Reena Kumari , Jagannath Nayak & A. Nityananda Shetty

To cite this article: P. D. Reena Kumari , Jagannath Nayak & A. Nityananda Shetty (2011) 3-Ethyl-4-amino-5-mercapto-1,2,4-triazole as a Corrosion Inhibitor for 6061/Al –15 vol% SiC_p Composite in a Sodium Hydroxide Solution, Synthesis and Reactivity in Inorganic, Metal-Organic, and Nano-Metal Chemistry, 41:7, 774-784, DOI: 10.1080/15533174.2011.591303

To link to this article: https://doi.org/10.1080/15533174.2011.591303

Published online: 11 Aug 2011.

Synthesis and Reactivity in Inorganic, Metal-Organic, and Nano-Metal Chemistry, 41:774–784, 2011

ISSN: 1553-3174 print / 1553-3182 online
DOI: 10.1080/15533174.2011.591303

Taylor & Francis
Taylor & Francis Group

3-Ethyl-4-amino-5-mercapto-1,2,4-triazole as a Corrosion Inhibitor for 6061/Al –15 vol% SiC_p Composite in a Sodium Hydroxide Solution

P. D. Reena Kumari,[1] Jagannath Nayak,[2] and A. Nityananda Shetty[1]

[1]*Department of Chemistry, National Institute of Technology Karnataka, Surathkal, Srinivasnagar, Mangalore, India*

[2]*Department of Metallurgical & Materials Engineering, National Institute of Technology Karnataka, Surathkal, Srinivasnagar, Mangalore, India*

The inhibition efficiency of 3-ethyl-4-amino-5-mercapto-1,2,4-triazole (EAMT) on the corrosion of 6061/Al–15 vol% SiC_p composite in different concentrations of sodium hydroxide solution has been investigated in the 30–50°C temperature range using Tafel and electrochemical impedance spectroscopic techniques. The inhibitor efficiency depends on the concentration of the inhibitor, concentration of the corrosive media, and temperature. The inhibition was assumed to occur through adsorption of the inhibitor molecule on the metal surface. The adsorption of the inhibitor on the metal surface is found to obey Langmuir adsorption isotherm. Thermodynamic parameters for the adsorption processes were determined from the experimental data.

Keywords Al–SiC_p composites, alkaline corrosion, electrochemical techniques, inhibition, triazole derivative

INTRODUCTION

Metal matrix composites, especially Al alloy matrices, have found widespread use in many engineering applications because of their high strength-to-weight ratio. The high thermal conductivity and low coefficients of thermal expansion of these materials have led to a number of applications that can involve exposure to potentially corrosive environment.[1–5] One of the main obstacles to the widespread incorporation of particulate MMCs into engineering applications is concern about the influence of reinforcement on corrosion resistance. This is of particular importance in aluminum alloy-based composites where corrosion resistance is imparted by a protective oxide film. The addition of a reinforcing phase could lead to further discontinuities or flaws in the film, increasing the sites for corrosion initiation and rendering the composite liable to severe attack.[6]

The use of inhibitors is one of the most common methods to protect metallic materials against corrosion in the environment containing aggressive ions. Due to the wide applications of aluminum composites, they frequently come in contact with caustic alkalies for cleaning, pickling, descaling, etc. As the dissolution rate of these composites in aqueous sodium hydroxide is very high, it may be desirable to inhibit the solution used for cleaning. The high corrosion rate of the composite materials in alkaline and acidic media can be combatted by using organic inhibitors. It has been reported that many organic compounds containing hetero atoms like N, O, and S and multiple bonds in their molecules have been proved to be effective inhibitors for the corrosion of aluminum alloys in acid and alkaline media.[7–14] Generally it has been assumed that the action of inhibitors in aggressive media is by the adsorption of the inhibitors onto the metal surface. The processes of adsorption of inhibitor are influenced by the nature and surface charge of the metal, the chemical structure of organic inhibitors, the type of aggressive electrolyte, and the type of interaction between organic molecules and the metallic surface.[15]

From the literature survey it is evident that there is no published information available on triazole derivatives as corrosion inhibitors for the aluminum composite material in alkaline media. The aim of this study is to investigate 3-ethyl-4-amino-5-mercapto-1,2,4-triazole (EAMT) as corrosion inhibitor for 6061 Al reinforced with 15 vol% SiC particulate composite in sodium hydroxide solution using potentiodynamic polarization and electrochemical impedance techniques. It is aimed at obtaining the information about surface morphology of the corroded composite metal by using scanning electron microscopy (SEM). It was also the purpose of this work to determine the thermodynamic parameters for the adsorption process and gain more information about the mode of adsorption of the inhibitor on the composite metal surface.

Received 18 October 2010; accepted 21 February 2011.

Address correspondence to A. Nityananda Shetty, Department of Chemistry, National Institute of Technology Karnataka, Surathkal, Srinivasnagar–575 025, Mangalore, India. E-mail: nityashreya@gmail.com

TABLE 1
The chemical composition of the base metal 6061 aluminum alloy

Element	Cu	Si	Mg	Cr	Al
Composition (wt%)	0.25	0.6	1.0	0.25	Balance

EXPERIMENTAL

Materials and Medium

The material employed was 6061/Al–15 vol% SiC_p composite in extruded rod form (extrusion ratio 30:1). The chemical composition of the base metal 6061 aluminum alloy is given in Table 1. Reinforced SiC has a mean particle diameter of 25 μm. The matrix of the composite has the purity of 99.8%. The sample was metallographically mounted up to 10 mm height using cold-setting epoxy resin, so that the exposed surface area of the metal to the media was 0.95 cm^2. The sample was mechanically polished using different emery papers up to 4/0 grades and finally polished on polishing wheel using levigated alumina. Then it was cleaned with acetone, washed with doubly distilled water, and finally dried. For the electrochemical measurement the arrangement used was a conventional three-electrode Pyrex glass cell with a platinum counter electrode and a saturated calomel electrode (SCE) as reference.

The test solution used for the investigation was standard solutions of sodium hydroxide prepared by using sodium hydroxide pellets of AR grade and double-distilled water.

Synthesis of EAMT

3-Ethyl-4-amino-5-mercapto-1,2,4-triazole was synthesized and recrystallized as per the reported procedure.[16] A mixture of thiocarbohydrazide (10 g) and propionic acid (60 mL) was heated, under reflux for 4 h. The product was recrystallized from ethanol and characterized by infrared (IR), elemental analysis, and melting point.

Potentiodynamic Polarization Method

Electrochemical measurements were carried out by using electrochemical work station, GillAC, and ACM Instruments Version 5 software. Tafel plot measurements were carried out using a conventional three-electrode Pyrex glass cell with platinum counter electrode and saturated calomel electrode (SCE) as reference electrode. All the values of potential are therefore referred to the SCE. Finely polished composite specimens were exposed to corrosion medium of different concentrations of sodium hydroxide at different temperatures (30 to 50°C) and allowed to establish a steady-state open circuit potential. The potentiodynamic current-potential curves were recorded by polarizing the specimen to –250 mV cathodically and +250 mV anodically with respect to open circuit potential (OCP) at a scan rate of 1 mV s^{-1}.

Electrochemical Impedance Spectroscopy Studies (EIS)

The corrosion behavior of the composite was also obtained from EIS technique using the electrochemical work station GillAC. In EIS technique a small-amplitude AC signal of 10 mV and frequency spectrum from 100 kHz to 0.01 Hz were impressed at the OCP and impedance data were analyzed using Nyquist plots. The polarization resistance was extracted from the diameter of the semicircle in the Nyquist plot.

In all the measurements just described, at least three similar results were considered and their average values are reported.

Scanning Electron Microscopy (SEM) Analysis

The scanning electron microscope images of the samples were recorded using a JEOL JSM–6380 LA analytical scanning electron microscope.

RESULTS AND DISCUSSION

Potentiodynamic Polarization Method

The polarization studies of the composite specimens were carried out in four different solutions containing 0.05 M, 0.1 M, 0.25 M, and 0.5 M sodium hydroxide, respectively, in the absence and in the presence of different concentrations of EAMT (5–100 ppm). Figure 1 shows the Tafel polarization curves of the composite in 0.5 M NaOH solution at 30°C devoid of and containing different concentrations of EAMT. Similar results were obtained in the same concentration of sodium hydroxide at four other temperatures and also in the other three concentrations of sodium hydroxide at the five temperatures studied. The electrochemical parameters (E_{corr}, i_{corr}, b_a, and b_c) associated with the polarization measurements at different EAMT concentrations as well as at different concentrations of the corrosion

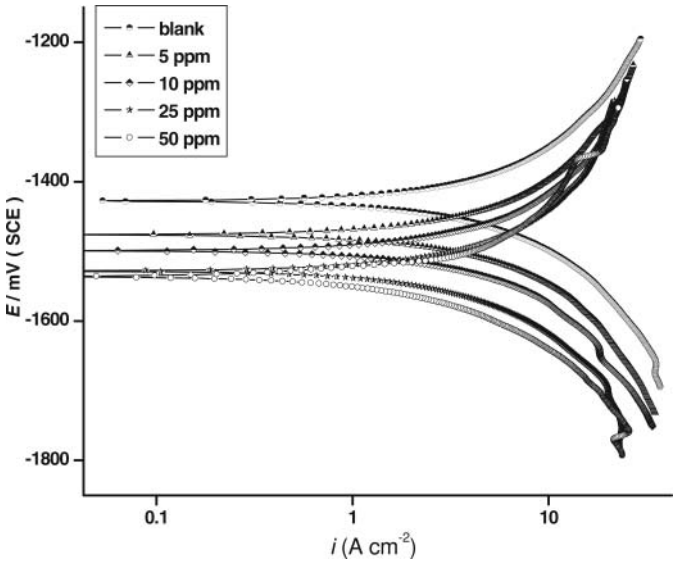

FIG. 1. Potentiodynamic polarization curves for 6061 Al/SiCp composite in 0.5 M NaOH at 30°C containing various concentrations of EAMT.

TABLE 2
Electrochemical parameters from polarization studies for 6061 Al/SiC_p composite with EAMT at 30°C in different concentrations of NaOH solutions

NaOH concentration (M)	Inhibitor concentration (ppm)	E_{corr} (mV/SCE)	b_a (mV dec^{-1})	$-b_c$ (mV dec^{-1})	i_{corr} (mA cm^{-2})	*IE* (%)
0.05	0	–1385	461	353	1.0758	—
	5	–1430	382	301	0.8756	16.12
	10	–1439	394	279	0.7856	24.79
	25	–1456	295	241	0.7299	30.12
	50	–1465	322	244	0.6959	36.61
	60	–1459	331	247	0.7026	34.70
	100	–1456	374	283	0.7400	31.20
0.1	0	–1406	403	335	1.9617	—
	5	–1459	254	235	1.2712	35.19
	10	–1475	240	210	1.2183	37.89
	25	–1494	195	177	0.9807	50.06
	50	–1503	193	165	0.7962	59.40
	60	–1500	198	166	0.7999	59.20
	100	–1481	242	208	0.8772	55.30
0.25	0	–1455	421	311	3.442	—
	5	–1477	181	169	2.351	31.68
	10	–1497	192	162	2.141	37.78
	25	–1517	192	171	1.897	44.88
	50	–1523	149	140	1.481	56.96
	60	–1518	154	148	1.508	56.20
	100	–1508	179	166	1.636	52.40
0.5	0	–1428	460	405	9.9459	—
	5	–1476	374	326	7.1239	28.37
	10	–1498	333	314	6.3219	36.43
	25	–1529	325	281	5.8691	40.98
	50	–1535	285	249	4.3126	56.63
	60	–1529	210	189	4.7747	55.30
	100	–1538	236	211	4.9639	50.10

media at 30°C for the composite are listed in Table 2. Similar results were obtained at other temperatures also.

The surface coverage θ is calculated as

$$\theta = \frac{i_{corr_{(uninh)}} - i_{corr_{(inh)}}}{i_{corr_{(uninh)}}}, \quad [1]$$

where $i_{corr(uninh)}$ and $i_{corr(inh)}$ are the corrosion current densities in the absence and presence of the inhibitor. The percentage of inhibition efficiency (*%IE*) is given by

$$\%IE = \theta \times 100. \quad [2]$$

The data in Table 2 clearly show that the addition of EAMT decreases the corrosion rates of the composite. Inhibition efficiency increases with increasing EAMT concentration up to a critical concentration and then decreases. It is also seen that the addition of EAMT shifts the E_{corr} values toward more negative potential, indicating cathodic inhibition action by EAMT. Further, it is seen from the data in the Table 2 that both the cathodic and anodic Tafel slopes change significantly on the addition of EAMT. These results indicate that EAMT acts as a mixed–type corrosion inhibitor with predominant control of cathodic reaction.[17] However, the results indicate that in the absence of inhibitor there is substantial corrosion of the composite in NaOH solution, and the corrosion rate increases with increase in concentration of the corrosion media. The presence of inhibitor brings down the corrosion rate considerably. Experimental data pertaining to inhibition efficiency of EAMT at different temperatures in the presence of different concentrations of inhibitors (data not shown in the article) also reveal that the inhibition efficiency decreases with increase in temperature for all concentrations of sodium hydroxide solution and also at all inhibitor concentration levels.

In alkaline solution the corrosion of aluminum could be explained by taking into account of the passive film, covering the

surface of aluminum.[18] In the strong alkaline medium, as used in the present study, the surface film readily dissolves, exposing the underlying aluminum atoms. The dissolution of aluminum atoms and gradual removal of these atoms through the formation of hydroxide, $Al(OH)_3$, takes place (Eq. 3). $Al(OH)_3$ species chemically reacts with OH^- ions to form a soluble aluminate ion, $Al(OH)_4^-$, that goes into the solution, leaving a bare metal site ready for another dissolution process.[19]

$$Al(m) + 3(OH)^- \rightleftarrows Al(OH)_3 \quad [3]$$

$$Al(OH)_3 + OH^- \rightleftarrows Al(OH)_4^- \quad [4]$$

The principal cathodic process is the reduction of water molecules to produce H_2 gas according to

$$H_2O_{(surface)} + e^- \rightleftarrows H + OH^- \quad [5]$$

$$H + H_2O_{(surface)} + e^- \rightleftarrows H_2 + OH^-. \quad [6]$$

The hydrogen overvoltage on aluminum is low, and therefore there is intense evolution of hydrogen when aluminum corrodes in NaOH solution. The inhibitor may affect either of the anodic and cathodic processes or both of them. From the experimental data it is clear that addition of EAMT considerably reduces aluminum dissolution process with a shift in the corrosion potential to the negative direction. Further inspection reveals that both anodic and cathodic Tafel slopes decrease upon addition of increasing concentrations of EAMT. This change in anodic and cathodic Tafel slopes in the presence of inhibitor shows that the latter affects both anodic and cathodic reactions. The corrosion current density is observed to be decreasing with increase in the concentration of the inhibitor, EAMT, up to a critical concentration. When the concentration of the inhibitor is increased above the critical concentration, the corrosion current density again increases. Accordingly, the inhibition efficiency of the inhibitor increases with the increase in the concentration of the inhibitor up to a critical concentration level and then decreases with further increase in the inhibitor concentration. The explanation for this trend is explained later in this article.

Electrochemical Impedance Spectroscopy (EIS) Studies

The corrosion behaviour of Al/SiC_p composite in all the conditions just described was also investigated by EIS. Figure 2 represents Nyquist plots of the composite in the presence of various concentrations of EAMT in 0.5 M NaOH at 30°C. Similar results were obtained in other three concentrations of NaOH and also at other temperatures studied.

As can be seen from Figure 2, the impedance diagrams show semicircles, indicating that the corrosion process is mainly charge transfer controlled and the additives do not change the reaction mechanism of the corrosion of composite in sodium hydroxide solution. The figure manifests two capacitive semicircles, separated by a small inductive loop at intermediate frequencies. The high frequency capacitive loop could be assigned to the charge transfer of the corrosion process and to the

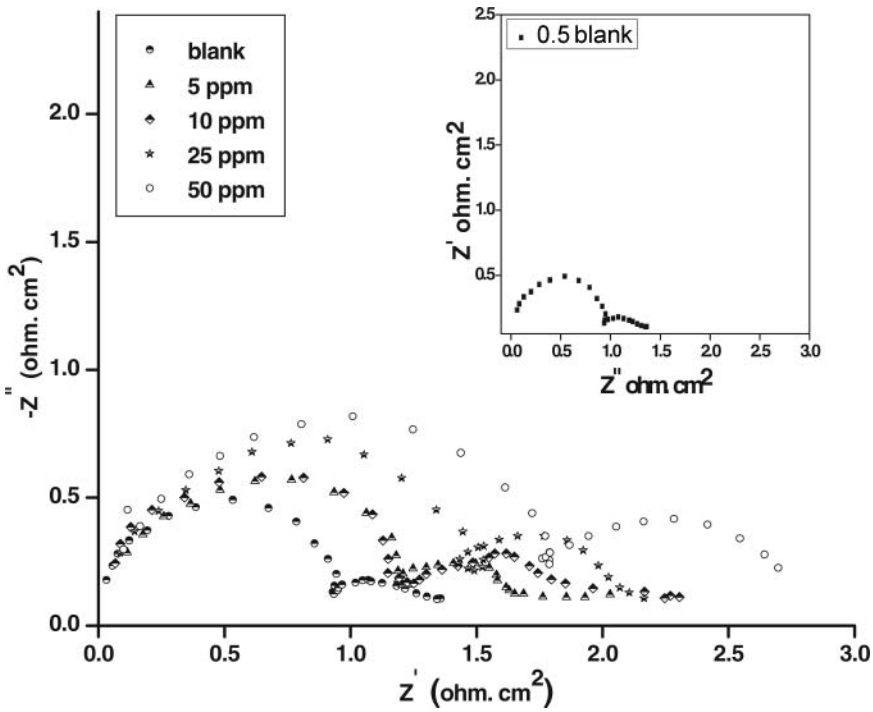

FIG. 2. Nyquists plots for 6061 Al/SiC_p composite in 0.5 M NaOH containing various concentrations of EAMT.

formation of oxide layer.[20] The oxide film is considered to be a parallel circuit of a resistor due to the ionic conduction in the oxide film and a capacitor due to its dielectric properties. According to Brett,[21] the capacitive loop is corresponding to the interfacial reactions, particularly the reaction of aluminum oxidation at the metal/oxide/electrolyte interface. The process includes the formation of Al^{+} ions at the metal/oxide interface, and their migration through the oxide/solution interface where they are oxidized to Al^{3+}. At the oxide/solution interface, OH^{-} or O^{2-} ions are also formed. The fact that all the three processes are represented by only one loop could be attributed either to the overlapping of the loops of processes, or to the assumption that one process dominates and therefore excludes the other processes.[22] The inductive loop may be related to the relaxation process obtained by adsorption of intermediates.[23] The low-frequency capacitive loop indicated the growth and dissolution of the surface film.

Two variations are observed on the impedance spectra in Figure 2. First, the high-frequency capacitive loop increases with the increase in EAMT concentration. The appreciation of the impedance can be attributed to the inhibition of the aluminum dissolution process due to the adsorption of EAMT on the composite surface. Second, the low-frequency capacitive loop increases with the increase in EAMT concentration. This is assumed to be due to the growth of the inhibitor surface film as the concentration of EAMT is increased.

The impedance data were analyzed using equivalent circuit (EC) model consisting of six elements as shown in Figure 3. In this equivalent circuit, R_s is the solution resistance, R_1 is the charge transfer resistance (R_{ct}), and L represents the inductive element. This also consists of a constant phase element, CPE (Q), in parallel to the parallel resistor R_1 and in series with R_2. There is also a capacitor element, C_1, in parallel with R_1.

The semicircles of the impedance spectra for the composite in the presence of the inhibitor are depressed. Deviation of this kind is referred to as frequency dispersion, and has been attributed to inhomogeneities of solid surfaces.[24] Mansfeld et al.[20] have suggested an exponent n in the impedance function as a deviation parameter from the ideal behavior. By this suggestion, the capacitor in the equivalent circuit can be replaced by a so-called constant phase element (CPE), which is a frequency-dependent element and related to surface roughness. The impedance function of a CPE has the following equation:[23]

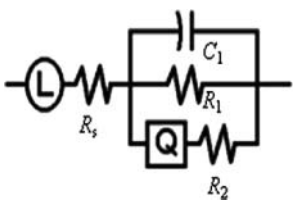

FIG. 3. The electrochemical equivalent circuit used for simulation of impedance data for 6061 Al/SiC_p composite in 0.5 M NaOH.

$$Z_{CPE} = Y_o^{-1}(j\omega)^{-n}, \quad [7]$$

where the amplitude Y_0 and n are frequency-independent CPE constant and exponent, respectively, and ω is the angular frequency in rad s^{-1} for which $-Z''$ reaches its maximum value, and $j^2 = -1$, an imaginary number; n is dependent on the surface morphology: $-1 \leq n \leq 1$. Y_0 and n can be calculated by the equations proved by Mansfeld et al.[25] In the absence of inhibitors the semicircle of the impedance spectra is more or less not depressed (shown in the inset of Figure 2), and this can be due to the high corrosion rate of the composite in NaOH solution. In the highly alkaline solution, the corrosion rate of aluminum is so high that it almost undergoes uniform corrosion, and therefore the surface inhomogeneity does not affect the Nyquist plot. In the presence of inhibitor, with the progressive formation of surface layer of the inhibitor, the corrosion rate decreases and surface no more remains uniform and homogeneous. Therefore, the effect of surface inhomogeneity comes into effect in depressing the semicircles of the Nyquist plots.

The double-layer capacitances C_{dl}, for a circuit including CPE were calculated from the following equation:[26]

$$C_{dl} = Y_o(2\pi f_{max})^{n-1}. \quad [8]$$

f_{max} is the frequency at which the imaginary component of the impedance is maximal. According to the expression of the double layer capacitance presented in the Helmholtz model:[27]

$$C_{dl} = \frac{\varepsilon\varepsilon_o}{d}S, \quad [9]$$

where d is the thickness of the film, S is the surface area of the electrode, ε_0 is the permittivity of air, and ε is the local dielectric constant. The value of C_{dl} decreases due to adsorption of inhibitor molecules, which displaces water molecules originally adsorbed on the alloy surface and decreases the active surface area. The value of double-layer capacitance decreases with increase in inhibitor concentration, indicating that inhibitor molecules function by adsorption at the metal/solution interface, leading to a protective film on the alloy surface, and decreasing the extent of dissolution reaction.[28] In accordance with the EC given in Figure 4, the polarization resistance R_p is given as

$$R_p = \frac{R_1 R_2}{R_1 + R_2}. \quad [10]$$

The percentage of inhibition efficiency,$\%IE$, was calculated from the following equation:

$$\%IE = \left[\frac{\left(\frac{1}{R_p}\right)_o - \left(\frac{1}{R_p}\right)}{\left(\frac{1}{R_p}\right)_o}\right], \quad [11]$$

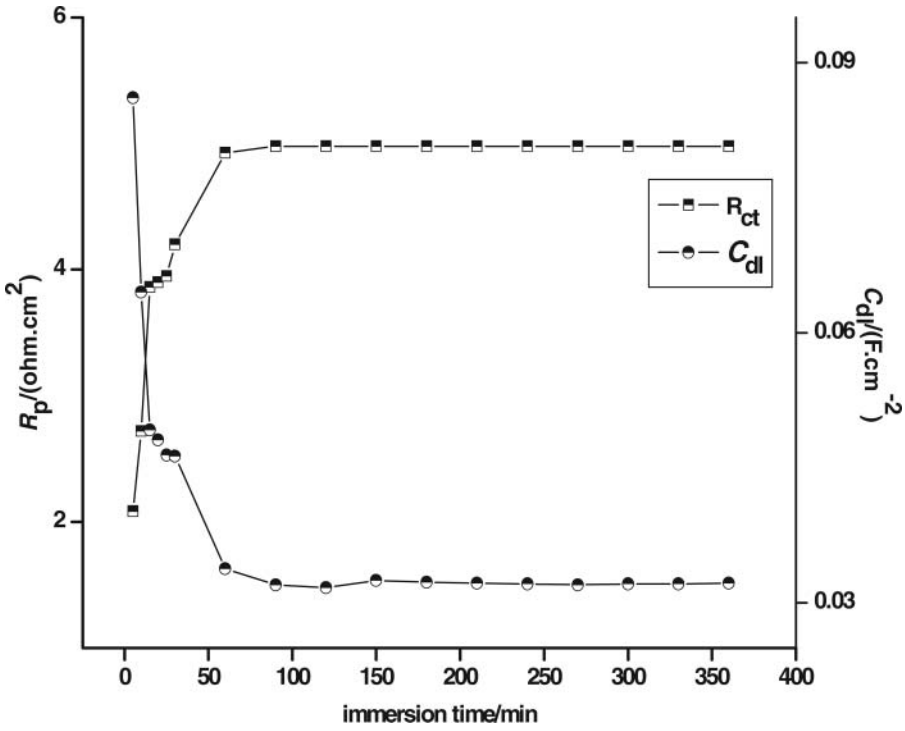

FIG. 4. The dependence of R_p and C_{dl} on the immersion time for 6061 Al/SiC$_p$ composite in 0.1 M NaOH containing 50 ppm of EAMT at 30°C.

where $(R_p)_o$ and (R_p) are the uninhibited and inhibited polarization resistances, respectively.

The impedance parameters derived from Nyquist plots and inhibition efficiency of EAMT in sodium hydroxide solutions of different concentrations in the presence of EAMT at various concentration levels at 30°C are given in Table 3. Similar results were obtained at other temperatures also. The measured values of polarization resistance (R_p) increase and those of the double-layer capacitance (C_{dl}) decrease with the increasing concentration of EAMT in the solution, indicating decrease in the corrosion rate for the composite with increase in EAMT concentration. This is in accordance with the observations obtained from potentiodynamic measurements.

From the results of Tafel studies and EIS studies, it is seen that the inhibition efficiency trend in different sodium hydroxide concentrations is 0.1 M > 0.25 M > 0.5 M > 0.05 M. As the concentration of sodium hydroxide increase, two factors come into operation, deciding the corrosion rate of the composite.[29] At higher concentrations of NaOH the inhibitor may readily ionize and be more easily adsorbed on the composite metal surface. At the same time, increasing sodium hydroxide concentration increases the corrosive power of the medium. At lower sodium hydroxide concentration, the first factor may be predominant over the second, and therefore, inhibition efficiency increases as the alkali concentration increase from 0.05 M to 0.1 M. At higher sodium hydroxide concentrations the second factor becomes more prominent, and therefore, above 0.1 M, further increase in the concentration of alkali in the solution decreases the inhibition efficiency.

Effect of the Immersion Time

Electrochemical impedance spectroscopy is a rapid and useful technique to evaluate the performance of the organic-coated metals R_p because they do not significantly disturb the system and it is possible to follow it overtime.[30] Therefore, more reliable results can be obtained from this technique and also it is possible to characterize the surface modification, i.e., formation and growth of inhibitor film.[31] Immersion time experiments were carried out in 0.1 M NaOH solution containing 50 ppm of EAMT for 360 minutes at 30°C, and Nyquist plots were recorded every 5 min during the initial 30 min, and then every 30 min afterward. The obtained results showed that the increase in immersion time increased the size of the capacitive loop and reaching a maximum in 90 min and remained fairly constant afterward. In Figure 4 the variation of both R_p and C_{dl} with the immersion time recorded for 0.1 M NaOH solution are shown graphically. Similar results were obtained for other concentrations of NaOH solutions also. It is obvious from the figure that R_p values increased sharply from 2.085 ohm cm^2 to 4.927 ohm cm^2 during the initial 60 min and remained fairly constant afterward. At the same time, C_{dl} values decreased up to 60 min and remained fairly constant thereafter. These results suggest that the formation of the inhibitive surface film on the electrode surface was almost completed within 60 min. These

TABLE 3
AC impedance data of 6061 Al/SiC_p composite with EAMT at 30°C in different concentrations of sodium hydroxide solution

NaOH concentration (M)	Inhibitor concentration (ppm)	R_p (ohm cm^2)	C_{dl} (F cm^{-2})	%IE
0.05	0	3.6721	0.0443	—
	5	4.1638	0.0372	11.8
	10	4.8274	0.0352	23.9
	25	4.8841	0.0309	24.8
	50	5.4406	0.0294	32.5
	60	5.3468	0.0295	31.3
	100	5.1210	0.0320	28.3
0.1	0	1.7627	0.0966	—
	5	2.6479	0.0799	33.4
	10	2.8884	0.0787	39.0
	25	3.3108	0.0649	46.8
	50	3.8863	0.0609	54.6
	60	3.8434	0.0652	54.1
	100	3.7832	0.0717	53.4
0.25	0	0.6153	0.1718	—
	5	0.9634	0.1286	36.1
	10	1.1570	0.0935	46.8
	25	1.1914	0.0837	48.4
	50	1.2730	0.0682	51.7
	60	1.2270	0.0711	49.9
	100	1.2080	0.0722	49.1
0.5	0	0.4172	0.2951	—
	5	0.5913	0.2797	29.4
	10	0.7048	0.2032	40.8
	25	0.7074	0.1595	41.0
	50	0.8371	0.1277	50.2
	60	0.8323	0.1339	49.9
	100	0.8089	0.1749	48.4

results demonstrate that the inhibition efficiency increases with increasing immersion time. This could be due to the progressive coverage of the composite surface by the compact adsorbed film of the inhibitor with time, with the EMAT anions being electrostatically adsorbed on the composite surface.

Adsorption Behavior

In order to understand the mechanism of corrosion inhibition, the adsorption behavior of the inhibitor molecules on the aluminum surface must be known. It is well known that adsorption isotherms provide useful insights into the characteristics of the adsorption process and the mechanism of corrosion inhibition.[32] The degree of surface coverage (θ) for different concentration of inhibitor was evaluated from potentiodynamic polarization measurements. The data were applied to different isotherm equations. It was found that the data fitted the Langmuir adsorption isotherm (Figure 5). According to

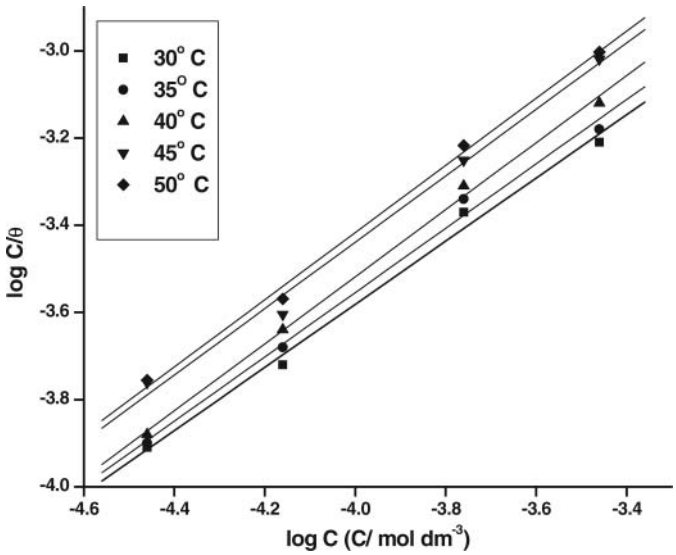

FIG. 5. Langmuir adsorption isotherm for the adsorption of EAMT.

the Langmuir adsorption isotherm, all the adsorption sites are equivalent, there are no interaction forces existing between the adsorbed molecules, and the energy of adsorption is independent of the surface coverage (θ).[33] The Langmuir adsorption isotherm could be represented by the equation:

$$\frac{C}{\theta} = C + \frac{1}{K}, \qquad [12]$$

where K is the adsorption/desorption equilibrium constant, C is the corrosion inhibitor concentration, and θ is the surface coverage.

The linear coefficient (R^2) was found to be close to unity, which has been used to select the best isotherm fitting the experimental data. The Langmuir isotherm plots in Figure 5 are linear, but the slopes are not equal to unity as would be expected for the ideal Langmuir adsorption isotherm equation. This deviation from unity may be due to the interaction among the adsorbed species on the metal surface. In the case of organic molecules, the polar groups or atoms are adsorbed at the anodic or cathodic sites of the metal surface. These adsorbed species may interact by mutual attraction or repulsion.[29] Thus, the inhibiting effect of EAMT molecules on composite metal surface in NaOH solution slightly deviates from ideal Langmuir adsorption isotherm.

The thermodynamic parameter, standard free energy adsorption, (ΔG°_{ads}) was calculated from the thermodynamic equation,

$$K = \frac{1}{55.5} \exp\left(\frac{-\Delta G^{\circ}_{ads}}{RT}\right), \qquad [13]$$

where K is the equilibrium constant for the adsorption/desorption process, 55.5 mol dm^{-3} is the molar concentration of water in the solution, T is temperature, and R is a gas

TABLE 4
Thermodynamic parameters for the adsorption of EAMT on 6061 Al/SiCp composite in NaOH solution at different temperatures

NaOH concentration (M)	Temperature (°C)	$-\Delta G^{\circ}_{ads}$ (kJ mol$^{-1)}$	$-\Delta H^{\circ}_{ads}$ (kJ mol^{-1})	$-\Delta S^{\circ}_{ads}$ (J mol^{-1} K^{-1})	log K	R^2
0.05	30	14.34	39.54	83.28	0.727	0.999
	35	13.76			0.588	0.998
	40	13.56			0.518	0.999
	45	12.83			0.363	0.999
	50	12.82			0.327	0.998
0.1	30	13.40	45.78	105.96	0.565	0.996
	35	13.38			0.524	0.998
	40	12.90			0.408	0.996
	45	11.97			0.222	0.995
	50	11.45			0.107	0.988
0.25	30	13.42	24.83	37.36	0.569	0.993
	35	13.38			0.524	0.997
	40	13.25			0.467	0.994
	45	12.93			0.379	0.992
	50	12.71			0.310	0.990
0.5	30	14.09	34.03	65.96	0.684	0.983
	35	13.84			0.603	0.983
	40	13.10			0.442	0.994
	45	13.01			0.392	0.998
	50	12.86			0.335	0.996

constant. Standard enthaply of adsorption (ΔH°_{ads}) and standard entropies of adsorption (ΔS°_{ads}) were obtained from the plot of (ΔG°_{ads}) versus T according to the thermodynamic basic equation:

$$\Delta G^{\circ}_{ads} = \Delta^{\circ}_{ads} - T\Delta S^{\circ}_{ads}. \quad [14]$$

The values of standard free energy of adsorption (ΔG°_{ads}), standard enthalpy of adsorption (ΔH°_{ads}), standard entropy for the adsorption process (ΔS°_{ads}), equilibrium constant (K), and linear correlation coefficient (R^2) obtained are given in Table 4 The negative values of ΔG°_{ads} indicate the spontaneity of the adsorption process and stability of the adsorbed layer on the metal surface. Generally the values of ΔG°_{ads} around –20 kJ mol^{-1} are consistent with physisorption, while those around -40 kJ mol^{-1} or higher involve chemisorptions.[34] The calculated values of ΔG°_{ads} obtained in this study (maximum value is 14.341 kJ mol^{-1}) indicate the physical adsorption behavior of EAMT on aluminum composite metal surface. The negative values of ΔH°_{ads} indicate that the adsorption of the inhibitor is an exothermic process. An exothermic adsorption process may involve either physisorption or chemisorption or a mixture of both processes.[35] From the ΔG°_{ads} values and the exothermic nature of the ΔH°_{ads}, it can be concluded that the adsorption of EMAT is physisorption. The ΔS°_{ads} values in the presence of inhibitor are negative, indicating that an increase in orderliness takes place on going from the free state to the adsorbed state of the inhibitors. This might be attributed to the orderly adsorption of the inhibitor molecules from a chaotic state of the freely moving molecules in the solution.[36]

Effect of Temperature and Activation Parameters

The change in the corrosion rate with increase in the temperature was studied for the composite material in NaOH solution without and with various concentrations of EAMT. It was observed that *%IE* increases with increase in the concentration of EAMT and decreases with increase in the temperature. The increase in temperature may cause desorption of the adsorbed EAMT molecules from the metal surface. The corrosion reaction could be approximated to an Arrhenius-type of process and the rate is given by

$$CR = k \exp\left(\frac{-E_a}{RT}\right), \quad [15]$$

where k is the Arrhenius preexponential factor and E_a is the activation energy of the corrosion process, R is the universal gas constant, and T is the absolute temperature. Arrehnius plots of ln *CR* versus 1/ *T* for the composite in 0.5 M NaOH solution in the absence and presence of various concentrations of EAMT are shown in Figure 6. From the slopes of the plots, activation energy values were calculated. The values of ΔH_a and ΔS_a were calculated from the plot of ln *CR*/*T* versus 1/*T* for aluminum composite in 0.5 M NaOH solution in the absence and presence

of various concentrations of EAMT according to the transition state equation:

$$CR = \frac{RT}{Nh} \exp\left(\frac{\Delta S_a}{R}\right) \exp\left(\frac{-\Delta H_a}{R}\right), \qquad [16]$$

where h is Planck's constant, N is Avogadro's number, ΔH_a is the activation enthalpy, and ΔS_a is the activation entropy. The calculated values of the apparent activation energy E_a, activation enthalpies ΔH_a, and activation entropies ΔS_a are given in Table 5.

These values indicate that the presence of additives increases the activation energy E_a and activation enthalpy ΔH_a and decreases activation entropy ΔS_a for the corrosion process. The increase in the activation energies with increasing concentration of the inhibitor is attributed to physical adsorption of inhibitor molecules on the metal surface,[37] with an appreciable increase in the adsorption process of the inhibitor on the metal surface with increase in the concentration of inhibitor. The adsorption of the inhibitor molecules on the surface of the alloy blocks the charge transfer during corrosion reaction, thereby increasing the activation energy.[38] In other words, the adsorption of the inhibitor on the electrode surface leads to the formation of a physical barrier that reduces the metal reactivity in the electrochemical reactions of corrosion.[39] The positive sign of the ΔH_a signifies the endothermic nature of dissolution process. The negative value of entropy of activation ΔS_a in the blank and

TABLE 5
Activation parameters for the corrosion of 6061 Al/SiC_p composite in NaOH solution in the absence and presence of different concentrations of EAMT

	Activation energy (kJ mol^{-1})				
NaOH concentration (M)	Blank	5 ppm	10 ppm	25 ppm	50 ppm
0.05	23.75	27.43	29.62	31.49	33.55
0.1	16.51	20.35	21.70	29.76	31.82
0.25	8.93	12.94	17.50	19.93	24.65
0.5	6.73	11.98	13.13	14.68	24.72
	ΔH_a(kj mol^{-1})				
0.05	21.15	24.82	27.02	28.89	30.95
0.1	13.91	17.75	19.10	27.16	29.72
0.25	6.33	10.34	15.53	17.33	22.10
0.5	4.13	9.38	10.53	12.08	22.12
	$-\Delta S_a$ (J mol^{-1} K^{-1})				
0.05	80.50	79.22	78.45	77.78	77.06
0.1	82.82	81.73	81.24	78.28	76.64
0.25	85.19	83.99	82.03	81.45	79.80
0.5	85.03	82.29	82.93	81.40	78.73

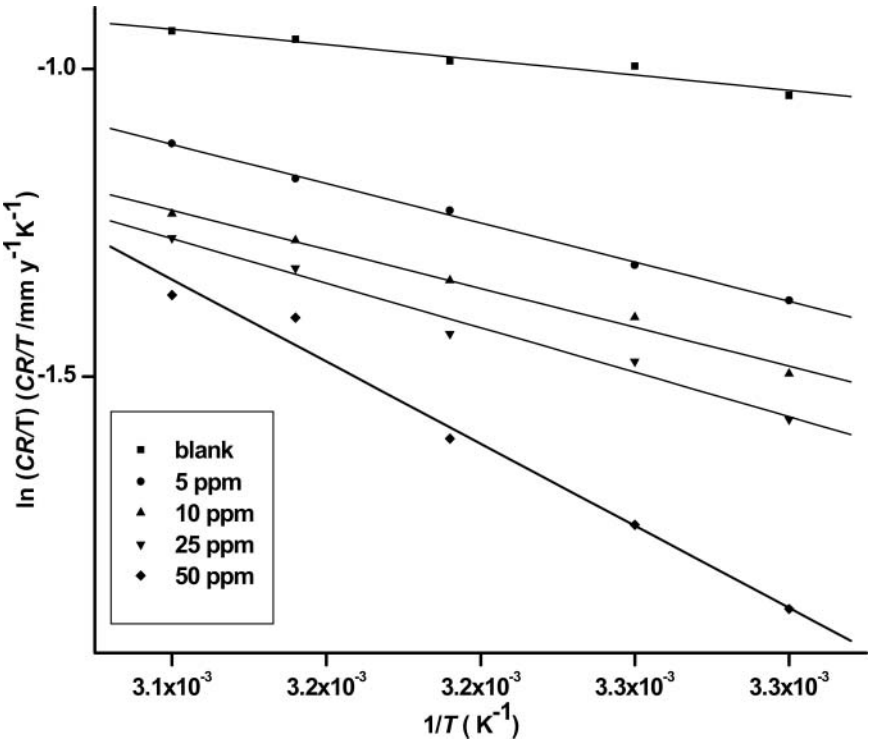

FIG. 6. Arrehnius plots for the corrosion of composite in 0.5 M NaOH in the presence and absence of EAMT.

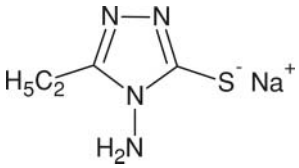

FIG. 7. Ionized form of EAMT in aqueous NaOH solution.

inhibited solutions implies that the formation of the activated complex is associated, with an increase in the order taking place in going from reactants to the activated complex.[40]

Inhibition Mechanism

Generally, the adsorption of organic molecules on metallic surfaces involves oxygen, nitrogen, and sulfur atoms as active centers, forming the linkages with the metal surface. The good inhibition efficiency of EAMT is attributed to strong adsorption of inhibitor species on the composite through the active centres, nitrogen and sulfur atoms. In NaOH solution EAMT exits in the ionized form as shown in Figure 7.

The presence of an ethyl group with + R (resonance) and + I (inductive) effects in the heterocyclic ring has a marked effect on the inhibition efficiency of the triazole molecule. A substituted ethyl group at the 3-position would donate charge through hyperconjugation and by the inductive effect, thus concentrating the charge density on nitrogen and sulfur atoms, thereby increasing their adsorption at the anodic sites of the metal that would normally suffer anodic attack. In the presence of aggressive hydroxide ions, it is assumed that the inhibitor anions with high charge density compete with anions such as OH^- ions (Eq. 3) and are preferentially adsorbed at the anodic sites of the metal surface. Adsorption of the inhibitor at the metal surface replaces the water molecules within the electrical double layer to produce a less pronounced dielectric effect[18] and thus holds up the reaction of surface water molecules according to Eqs. (5) and (6); thus the rate of hydrogen evolution is reduced, thereby affecting the cathodic reactions.

Scanning Electron Microscopy

In order to evaluate the surface morphology of the 6061 Al/SiC_p composite surface in contact with alkaline solution, a superficial analysis was carried out. The SEM micrograph of the corroded specimen after 1 h of immersion in 0.5 M NaOH solution is shown in Figure 8(a). The faceting seen in the figure is due to the attack of aggressive hydroxide ions on the composite sample, causing more or less uniform corrosion. Figure 8(b) depicts the SEM of the specimen after 1 h of immersion in 0.5 M NaOH solution with the addition of 50 ppm EAMT. It can be seen that the flakes on the surface of the specimen are reduced when compared with the micrograph given in Figure 8(a). The specimen surface can be observed to be covered with a thin layer of the inhibitor molecules, giving protection against corrosion.

CONCLUSIONS

- The corrosion studies of the 6061 Al/SiC_p composite were carried out at 30 to 50°C temperatures using NaOH solutions and the results indicate that EAMT improved the corrosion resistance of the composite in alkaline environment.
- Inhibition efficiency of EAMT initially increases as the concentration of NaOH increases from 0.05 M to 0.1 M and then decreases on further increase in the concentration of NaOH.
- Inhibition efficiency decreases with increase in temperature of the medium.
- The potentiodynamic polarization curves suggest a mixed type with predominantly control of cathodic reaction for the inhibition process in NaOH solution.
- The adsorption of EAMT on the composite metal surface follows a Langmuir adsorption isotherm with the slight deviation from the ideal Langmuir adsorption isotherm behavior, showing interaction among the adsorbed species.

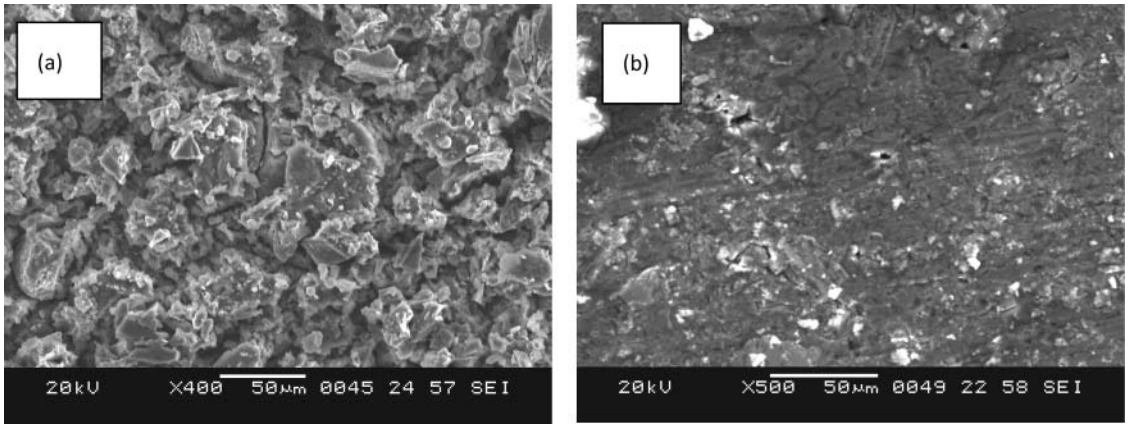

FIG. 8. SEM image of surface of 6061 Al/SiC_p composite after immersion for 1 h in 0.5 M NaOH solution at 30°C (a) in the absence of EAMT and (b) in the presence of 50 ppm EAMT.

- The inhibition efficiency obtained from potentiodynamic polarization and that obtained from EIS techniques are in reasonably good agreement.

REFERENCES

1. Candan, S.; Biligic, E. Corrosion behavior of Al–60 vol.% SiCp composites in NaCl solution. *Mater. Lett.* **2004**, *58*, 2787–2790.
2. Bakkar, A.; Neubert, V. Corrosion characterisation of alumina–magnesium metal matrix composites. *Corros. Sci.* **2007**, *49*, 1110–1130.
3. Griffiths, A.J.; Turnbull, A. An investigation of the electrochemical polarization behaviour of 6061 aluminum metal matrix composites. *Corros. Sci.* **1994**, *36*, 23–35.2
4. Mansfeld, F.; Jeanjaquet, S.L. The evaluation of corrosion protection measures for metal matrix composites. *Corros. Sci.* **1986**, *9*, 727–734.
5. Gul, T.; Mehtap, M. The drilling of Al/SiCp metal-matrix composites. Part II: Work pièce surface integrity. *Compos. Sci. Technol.* **2004**, *64*, 1413–1418.
6. Trowsdale, A.J.; Noble, B.; Harris, S.J.; Gibbins, I.S.R.; Thompson, G.E.; Wood, G.C. The influence of silicon carbide reinforcement on the pitting behaviour of aluminium *Corros. Sci.* **1996**, *2*, 177–191.
7. Talati, J.D.; Modi, R. M. *p*-Substituted phenols as corrosion inhibitors for aluminium-copper alloy in sodium hydroxide. *Corros. Sci.* **1979**, *19*, 35–48.
8. Muller, B. Corrosion inhibition of different metal pigments in aqueous alkaline media. *Corros. Sci.* **2001**, *43*, 1155–1164.
9. Maayta, A.K.; Al-Rawashdeh, N.A.F. Inhibition of acidic corrosion of pure aluminium by some organic compounds. *Corros. Sci.* **2004**, *46*, 1129–1140.
10. Maayta, A.K. Organic corrosion inhibitors for aluminium in sodium hydroxide. *J. Corros. Sci. Eng.* **2002**, *3*(*25*), 1–7.
11. Henryk, S.; Martin, M.D.J. The applications of 1-hydroxyimidazole-3-N-oxides as aluminium corrosion inhibitors in alkaline solutions. *Corros. Sci.* **1992**, *12*, 1967–1992.
12. Bereket, G.; Pinarbasi, A. Electrochemical thermodynamic and kinetic studies of the behavior of aluminium in hydrochloric acid containing various benzotriazole derivatives *Corros. Eng. Sci. Technol.* **2004**, *39*, 308–312.
13. Mohammed, K.A. Semiempirical investigation of the inhibition efficiency of thiourea derivatives as corrsion inhibitors. *J. Electroanal. Chem.* **2004,** *67*, 219–225.
14. Zheludkevich, M.L.; Yasakau, K.A.; Poznyak, S.K.; Ferreria, M.G.S. Triazole and thiazole derivatives as corrosion inhibitors for AA2024 aluminium alloy. *Corros. Sci.* **2005**, *47*, 3368–3383.
15. Abdallah, M. Antibacterial drugs as corrosion inhibitors for corrosion of aluminium in hydrochloric solution. *Corros. Sci.* **2004**, *46*, 1981–1996.
16. Shah, P.T.; Daniels, T.C. *Rev. Trav. Chim.* **1950**, *69*, 1545–1551.
17. Yurt, A.; Ulutas, S.; Dal, H., Electrochemical and theoretical investigation on the corrosion of aluminium in acidic solution containing some schiff bases. *Appl. Surf. Sci.* **2006**, *253*, 919–925.
18. Lorenz, W.J.; Mansfeld, F. Determination of corrosion rates by electrochemical DC and AC methods. *Corros. Sci.* **1981** , *21*, 647–672.
19. Al- Kharafi, F.M.; Badawy, W.A. Inhibition of corrosion of Al 6061, aluminium, and an aluminium-copper alloy in chloride-free aqueous media: Part 2. Behavior in basic solutions. *Corrosion* **1997**, *5*, 377–385.
20. Mansfeld, F.; Lin, S.; Kim, S.; Shih, H. Pitting and surface modification of SiC/Al. *Corros. Sci.* **1987**, *27*, 997–1000.
21. Brett, C.M.A. The application of electrochemical impedance techniques to aluminium corrosion in acidic chloride solution. *J. Appl. Electrochem.* **1990**, *20*, 1000.
22. Wit, J.H.; Lenderink, H.J.W. Electrochemical impedance spectroscopy as a tool to obtain mechanistic information on the passive behaviour of aluminium. *Electrochim. Acta* **1996**, *41*, 1111–1119.
23. Lenderink, H.J.W.; Linden, M.V.D.; De Wit, J.H.W. Corrosion of aluminium in acidic and neutral solutions. *Electrochim. Acta* **1993**, *38*, 1989–1992.
24. Jutner, K. Electrochemical impedance spectroscopy of corrosion processes on inhomogeneous surfaces. *Electrochim. Acta* **1990**, *35*, 1501–1508.
25. Mansfeld, F.; Tsai, C.H.; Shih, H. In Munn, R.S. (ed.), *Computer Modeling in Corrosion*; ASTM: Philadelphia, **1992**, p. 197.
26. Hsu, C.H.; Mansfeld, F. Concerning yhe conversion of constant phase element parameter into a capacitance. *Corrosion* **2001**, *57*, 747–748.
27. McCafferty, E.; Hackerman, N. Kinetics of Iron corrosion in concentrated acidic chloride solutions. *J. Electrochem. Soc.* **1972**, *119*, 999–1009.
28. Bentiss, F.; Traisnel, M.; Lagrenee, M. The substituted 1,3,4-oxadiazoles: A new class of corrosion inhibitors of mild steel in acidic media. *Corros. Sci.* **2000**, *42*, 127.
29. Bansiwal, A.; Anthony, P.; Mathur, S.P. Inhibitive effect of some Schiff bases on corrosion of aluminium in hydrochloric acid solutions. *Br. Corros. J.* **2000**, *4*, 301–303.
30. Dehri, I.; Erbil, M. The effect of relative humidity on the atmospheric corrosion of defective organic coating materials: An EIS study with a new approach. *Corros. Sci.* **2000**, *42*, 969–978.
31. Solmaz, R.; Kardas, G.; Culha, M.; Yazici, B.; Erbil, M. Investigation of adsorption and inhibitive effect of 2-mercaptothiazoline on corrosion of mild steel in hydrochloric acid. *Electrochim. Acta* **2008**, *53*, 5941–5952.
32. Durnie, W.; De Marco, R.; Jefferson, R.; Kinsella, B. Development of a structure–activity relationship for oil field corrosion inhibitors. *J. Electrochem. Soc.* **1990**, *146*, 1751–1756.
33. Rosiliza, R.; Wan Nik, W.B. Improvement of corrosion resistance of AA6061 alloy by tapioca starch in seawater. *Curr. Appl. Phys.* **2010**, *10*, 221–229.
34. Umoren, S.A.; Ebenso, E.E.; Okafor, P.C.; Ekpe, U.J.; Ogbobe, O. Effect of halide ions on the corrosion inhibition of aluminium in alkaline medium using polyvinyl alcohol. *J. Appl. Polym. Sci.* **2007**, *103*, 2810–2816.
35. Khadom, A.A.; Yaro, A.S.; Al Tafie, A.S.; Kadum, A.A.H. Electrochemical activations and adsorptions studies for the corrosion inhibition of low carbon steel in acidic media. *Portugal Electrochim Acta* **2009**, *27*, 699–712.
36. Libin, T.; Guannan, M.; Guangheng, L. The effect of neutral red on the corrosion inhibition of cold rolled steel in 1.0 M hydrochloric acid. *Corros. Sci.* **2003**, *45*, 2251–2262.
37. Ashassi-Sorkhabi, H.; Shaabani, B.; Seifzadeh, D. Corrosion inhibition of mild steel by some Schiff base compounds in HCl. *Appl. Surf. Sci.* **2005**, *239*, 154–164.
38. Osman, M.M.; El-Ghazawy, R.A.; Al-Sabagh, A.M. Corrosion inhibitor of some surfactants derived from maleic-oleic acid adduct on mild steel in 1 M H_2SO_4. *Mater. Chem. Phys.* **2003**, *80*, 55–62.
39. Mansfeld, F. *Corrosion Mechanism*; Marcel Dekker: New York, **1987**.
40. Satpati, A.K.; Ravindran, P.V. Electrochemical study of the inhibition of corrosion of stainless steel by 1, 2, 3- benzotriazole in acidic media. *Mater. Chem. Phy.* **2008**, *109*, 352–359.